Title: The structure of Rns from enterotoxigenic *Escherichia coli* reveals a small molecule inhibitor

Authors: Charles R Midgett[1#], Kacey Marie Talbot[2#], Jessica L. Day[1,3], George P Munson[2], and F Jon Kull[1$]

Affiliations:
1 Department of Chemistry, Dartmouth College, Hanover, NH
2 Department of Microbiology and Immunology, Miller School of Medicine, University of Miami, Miami, FL
3 Department of Biochemistry, Geisel School of Medicine at Dartmouth, Hanover, NH

# These authors contributed equally to this work
$ Corresponding Author: F Jon Kull, f.jon.kull@dartmouth.edu

Abstract

Infections caused by the gram-negative bacteria enterotoxigenic *Escherichia coli* (ETEC), *Vibrio cholerae*, *Shigella flexneri*, and *Salmonella enterica* are among the most common enteric pathogens and infect billions of people each year. These bacteria control expression of virulence factors using a genetic network of transcriptional regulators, some of which are modulated by small molecules as has been shown for ToxT, an AraC family member from *V. cholerae*. In ETEC the expression of many types of adhesive pili is dependent upon the AraC family member Rns. We present here the 3 Å crystal structure of Rns and show it closely resembles ToxT. Furthermore, Rns contains a ligand, decanoic acid, that inhibits its activity in a manner similar to the fatty acid mediated inhibition observed for ToxT and the *S. enterica* homologue HilD. Rns crystallized as a dimer via an interface similar to that observed in other dimeric AraC's. Together, these results support our hypothesis that virulence controlling AraC family members are regulated by fatty acids in a common manner in a number of enteric pathogens. Furthermore, for the first time this work identifies a small molecule capable of inhibiting ETEC virulence, providing a basis for development of therapeutics against this deadly human pathogen.

Introduction

Diarrheal diseases are estimated to cause nearly 1.3 million deaths every year (Troeger *et al.*, 2017). Enterotoxogenic *E. coli* (ETEC) is leading cause of diarrhea, however there are very different estimates of its prevalence. Older estimates suggested 280 million global infections with 380,000 deaths per year of children under five (World Health Organization, 1999), while newer estimates suggest only 75 million cases each year, killing up to 30,659 children under the age of five (Khalil *et al.*, 2018). While there is debate about the worldwide incidence of ETEC it is clearly a leading cause of traveler's diarrhea and is of particular concern during military deployments (Jiang and DuPont, 2017; Porter *et al.*, 2017).

ETEC colonization is dependent on production of pili, sometimes referred to as colonization factors, that are required for the bacteria to attach to the intestinal wall. In the absence of adhesive pili, ETEC is unable to cause infection (Turner *et al.*, 2006). Over 20 of these highly immunogenic colonization factors have been identified (Fleckenstein and Kuhlmann, 2019), and while it has been hypothesized vaccines incorporating them could be protective from ETEC infection (Boedeker, 2005; Vidal *et al.*, 2019), to date such vaccines have failed to induce immunity (Boedeker, 2005). This coupled with the rise of antibiotic resistant strains, with their associated treatment challenges and increased cost (Shakoor *et al.*, 2019), shows it is critical to change vaccine strategy, as well as identify new avenues for treatment.

While ETEC colonization factors are diverse, nearly half are regulated by the transcription factor Rns (also known as CfaD or CfaR), a member of the AraC family (Caron *et al.*, 1989; Caron *et al.*, 1990; Maria Del Tocio Bodero *et al.*, 2008; Munson, 2013). Rns activates pilin promoters by binding to a proximal site immediately adjacent to the -35 hexamer (Munson and Scott, 1999; Munson and Scott, 2000; Maria Del Rocio Bodero *et al.*,

2007), which may be accompanied by one or more additional sites further upstream. Like most other AraC family members, Rns contains two helix-turn-helix DNA binding motifs in its carboxy terminal domain (Gallegos *et al.*, 1997), as well as an amino terminal domain that has been suggested to be involved in dimerization (Mahon *et al.*, 2010) and ligand binding (Gallegos *et al.*, 1997). Notably, prior to this study ligand binding by Rns has not been experimentally demonstrated.

ToxT, an AraC family member from *V. cholerae* regulates transcription of the two major virulence factors, the toxin-coregulated pilus (TCP) and cholera toxin (CT) (DiRita *et al.*, 1991; Higgins *et al.*, 1992). Previous work in our laboratory identified unsaturated fatty acids (UFAs) inhibit ToxT activity through binding a pocket in the N-terminal domain. This inhibition is potentially due to a disruption in the ability of ToxT to bind to promoter sites as the presence of the monounsaturated fatty acids oleic (C18) and palmitoelic (C16) acids inhibited ToxT DNA binding *in vitro* (Lowden *et al.*, 2010). As fatty acids are a component of bile, which is present in the GI tract of most organisms affected by *V. cholerae*, it is reasonable that such compounds would make an effective signal for virulence regulation (Chatterjee *et al.*, 2007) and suggests other virulence controlling AraC family members might be inhibited by a similar mechanism (Lowden *et al.*, 2010). A computational screen of AraC proteins identified several candidates for such regulation, including Rns.

In order to determine whether Rns is inhibited by UFA's in a manner similar to ToxT, we solved the crystal structure of Rns. We observed two protein conformations, "open" and "closed" and show that Rns forms a dimer, consistent with it binding DNA as a dimer in a manner similar to other AraC proteins (Soisson *et al.*, 1997; LaRonde-LeBlanc and Wolberger, 2000; Shrestha *et al.*, 2015). Inspection of the open conformation revealed an unknown ligand bound in a groove between the N- and C-terminal domains, which was modeled as decanoic acid. Differential scanning fluorometry revealed decanoic acid increased the melting temperature (T_m) of Rns, stabilizing it and supporting a model in which decanoic acid binds specifically. When Rns was crystallized with excess decanoic acid only the closed conformation was observed. In support of a physiological role for a fatty acid ligand, exogenous decanoic acid abolished the expression of colonization factors by inhibiting Rns-dependent transcriptional regulation. These results support the hypothesis that Rns, like ToxT, utilizes a common mechanism of binding fatty acid effector molecules to regulate virulence gene expression.

Materials and Methods

Identification of candidate AraC proteins

Fifty-eight proteins that had been previously characterized and identified as AraC family members were chosen for analysis (Ibarra *et al.*, 2008). Although these proteins were linked to various functions (categories included: general metabolism, adaptive responses to nutrient sources, stress, and virulence), we analyzed all 58, regardless of functional class. As the prior study utilized sequence alignments for their analysis (Ibarra *et al.*, 2008), we used alignments of the predicted secondary structure for our analysis. The following criteria were used to identify possible candidates: 1) The protein length was similar to that of ToxT.

2) The predicted secondary structure indicated a protein with an N-terminal β-strand rich domain and a C-terminal DNA binding domain comprised of seven α-helices (the canonical AraC DNA binding domain). 3) The presence of a positively charged amino acid at the C-terminal end of the α-helix predicted to be analogous to Lys230 in α7 of ToxT. 4) The presence of a positively charged amino acid in an appropriate position in the β-strand N-terminal domain. As β-strands are much more difficult to predict than α-helices, and as β-strand domains are inherently more variable, the exact location of this residue was more flexible than in rule #3. Using these rules, we identified four AraC virulence regulators out of the 58 that met all four primary criteria and for which comparison with an existing phylogenic tree(Ibarra *et al.*, 2008) showed they were among the closest relatives of ToxT. From members of the initial 58 candidates that failed our virtual screen based on rule #3, we identified three additional AraC proteins that are involved in virulence and have a positively charged residue near the end of the helix (Fig. 1, Table 1).

Cloning of Rns into an expression vector

The sequence encoding Rns was optimized to remove rare codons, and flanking sequences to insert into the plasmid pCDB24, a gift from Dr. Bahl (Institute for Protein Innovation), which contains a N-terminal 10xHis-SUMO tag (pCDB24 addgene.org), were added. The resulting construct was synthesized by IDT. The construct sequence was amplified using PCR and the resulting product was purified using the QIAquick PCR purification kit from Qiagen. The vector was digested with XhoI and purified using the QIAqucik PCR purification kit. The *rns* construct was cloned into the digested vector in frame with the SUMO tag, using the DNA Assembly Mix from NEB according to the manufacturer's instructions, to create the 10xHis-SUMO-Rns (SMT-Rns) construct. The correct insertion of *rns* was verified by sequencing. The resulting plasmid was transformed into BL21 DE3 cells for unlabeled protein expression and into B834 DE3 cells for SeMet labeling.

SeMet labeled protein expression

SeMet labeled protein was expressed using Selenomet media from Molecular Dimensions. The cultures were initiated from a frozen stock into Selenomet media supplemented with 50 μg/ml of L-methionine and 100 μg/ml carbenicillin. The culture was incubated at 37 ºC overnight with shaking. The next morning the culture was centrifuged at 25 ºC for 10 mins at 3000 xg to collect the cells. The cells were washed three times with water. After washing the cells were resuspended in a 10 fold larger volume of Selenomet media supplemented with 50 μg/ml of seleno-L-methionine, and 50 μg/ml of carbenicillin. The culture was incubated at 37 ºC till an OD600 of 1-2. The culture was induced by adding 500 μM IPTG and incubated at 18 ºC overnight.

Unlabeled Rns expression

SMT-Rns was expressed in modified TB media (Fisher Scientific). To start a frozen stock was used to inoculate a starter culture of 2 ml ZYP-0.8G media (ZYP media (Studier, 2005) supplemented with 0.8% glucose) with 200 μg/ml carbenicillin, which was incubated overnight at 30 ºC. The next morning of the starter was diluted 1:100 in TB containing 2 mM $MgSO_4$ and 200 μg/ml of carbenicillin. This culture was incubated at 37 ºC till an OD600 of

2-3. The culture then diluted 1:10 in TB with 2 mM $MgSO_4$ and 50 μg/ml carbenicillin in a 3 L baffled flask. This was again incubated at 37 ºC till it reached an OD600 of 2-3. The culture was then induced with 500 μM IPTG and 5% glycerol was added. The culture was incubated at 18 ºC overnight.

Rns purification

SMT-Rns purification was performed as follows. The culture was pelleted at 3000 xg for 25 mins. The bacteria were resuspended in wash buffer (20 mM TRIS pH 8, 20 mM imidazole, 500 mM NaCl) supplemented with 500 μM EDTA, 500 μM PMSF, and a Roche protease inhibitor tablet. The culture was lysed by three passes through a French press. The lysate was clarified by ultracentrifugation at ~100,000 x g for 45 mins. The supernatant was filtered using a 0.45 μm filter, and 1 M $MgCl_2$ was added to a final concentration of 1 mM.

The SMT-Rns was captured using a HisTrap column from GE Healthcare. The column was equilibrated with 10 CV of elution buffer (20 mM TRIS pH 8, 500 mM imidazole, 500 mM NaCl) followed by 10 CV of wash buffer. The supernatant was loaded onto the column at 2 ml/min. The column was washed with 10 CV of wash buffer followed by 9 CV of 9% elution buffer, and 2 CV of 20% elution buffer. SMT-RNS was eluted from the column with a 10 CV gradient of 20%-100% elution buffer. Fractions were collected in tubes with EDTA for a final concentration of 100 μM.

Cleavage of the SMT-Rns was achieved using previously purified 6xHis-Ulp1-6xHis SUMO protease, a gift from Dr. Bahl (Institute for Protein Innovation). The relevant fractions from the His-Trap column were pooled and dialyzed against 2 L of (20 mM TRIS pH 8, 200 mM NaCl, 1 mM DTT, 500 μM EDTA) at 4 ºC. After ~4 hours the dialysis buffer was changed, and a 10 mg aliquot of the protease was added to the pooled fractions. Dialysis was continued overnight at 4 ºC. The next morning a HisTrap column was equilibrated with 5 CV of dialysis buffer with 1 mM $MgCl_2$ and 20 mM imidazole. Imidazole was added to the dialysate for a final concentration of 20 mM and $MgCl_2$ was added for a final concentration of 1 mM. The dialysate was then applied to the column and the flow through was collected.

Final purification was carried using an HiTrap Sp ion exchange column (GE Healthcare). The column was equilibrated with 10 CV of Sp elution buffer (20 mM TRIS pH 8, 1 M NaCl, 250 μM EDTA) followed by 10 CV of Sp wash buffer (20 mM TRIS pH 8, 200 mM NaCl, 250 μM EDTA). Then the flow through from the cleavage step was loaded onto the Sp column. The column was washed with 10 CV of Sp wash buffer. Elution was performed using a gradient to 100% Sp elution buffer over 5 CV. The concentrations of the relevant fractions were determined, and DTT to a final concentration of 1 mM was added to the fractions.

Crystallization and data collection

Initial crystal screening for the SeMet labeled Rns was done using 96 well block screens from either Qiagen or Hampton Research. Initial drops were setup either at 2 mg/ml or 0.6 mg/ml using a NT8 robot. The crystals were imaged using Rock Imager. The initial hits were then optimized. The best crystals of Rns were obtained in a base condition of 0.1

M (D/L) malic acid pH 7, with 6%-10% PEG 3350. These conditions were then used in additive screens, Additive Screen (Hampton Research). The final crystallization condition for SeMet labeled Rns was .6 mg/ml protein added 1:1 to 0.1 M (D/L) malic acid pH 7, 6% PEG 3350, 0.01 M Betaine hydrochloride in sitting drops. The crystals were frozen using the well solution supplemented with 10% PEG 3350, and 40% glycerol as the cyro-protectant. Data was collected using the FMX beam line at NSLS-II. Two anomalous data sets were collected from the same crystal with 360º of rotation at a wavelength of 0.979184 Å.

Another set of screens were setup with native Rns at .6 mg/ml with 1 mM decanoic acid. The native Rns, decanoic acid mix was crystallized by adding the mixture in a 1:1 ratio to 0.1 M succinnic acid, 14% PEG 3350, 0.03 M glycyl-glycyl-gylcine in hanging drops. The crystals were frozen with the well solution supplemented with 30% ethylene glycol as the cryo-protectant. Diffraction data was collected at the AMX beam line at NSLS-II.

Anomalous data processing and refinement

The anomalous data sets were processed using XDS (Kabsch, 2010). The space group was determined to be P 2_1 with a unit cell of 72.51, 49.97, 102.92, 90.00, 106.11, 90.00. The two datasets were combined in XSCALE (Kabsch, 2010). The processed data was cut at 2.8 Å and used in a Hybrid Substructure Search followed by one round of AutoSol and one round of AutoBuild in PHENIX (Adams *et al.*, 2010). The model was refined using iterative rounds of automated refinement with Refine as implemented in PHENIX with NCS, secondary structure, as well as experimental phase restraints (Adams *et al.*, 2010), followed by manual model building using COOT (Emsley and Cowtan, 2004). Chimera and Chimerax were used for model visualization (Pettersen *et al.*, 2004; Goddard *et al.*, 2017). Refinement statistics are listed in Table 2.

Native data processing and refinement

The native data sets were processed using XDS (Kabsch, 2010). The space group was $P2_12_12_1$ with a unit cell of 48.24 95.15 133.09 90 90 90. This crystal had significant pseudo-translational symmetry with an off-origin peak 46% of the origin peak as determined by PHENIX (Adams *et al.*, 2010). The structure was solved using Phaser (McCoy *et al.*, 2007) as implemented in PHENIX (Adams *et al.*, 2010)using the previously solved SeMet-Rns as a search model. After phaser there was visible density in the ligand binding pockets of both monomers. The density was still visible after a cycle of automated refinement in PHENIX (Adams *et al.*, 2010). Decanoic acid was added to the density using COOT (Emsley and Cowtan, 2004) and refinement was performed using iterative rounds of PHENIX Refine (Adams *et al.*, 2010) followed by manual model building in COOT (Emsley and Cowtan, 2004). Chimera and Chimerax were used for model visualization (Pettersen *et al.*, 2004; Goddard *et al.*, 2017). Refinement statistics are listed in Table 2.

Differential scanning fluorometry (DSF)

DSF was performed to assess the effect of fatty acids on Rns stability (Niesen *et al.*, 2007). First stocks of fatty acids at 10x of final concentration were made by adding octanoic, decanoic, and palmitic acid to methanol. The samples were made by adding buffer with the Sypro Orange dye (Life Technologies) to a PCR plate (final Sypro Orange concentration

5x). Then the fatty acids were added to the tubes. Finally, Rns was added to the tubes to a final concentration of .7 mg/ml. The melting curves were generated using a StepOne + RT PCR machine (Life Technologies) with a gradient from 25 ºC to 95 ºC utilizing 1 ºC steps. The normalized melt data was exported into STATA for analysis as described (Midgett *et al.*, 2017).

Plasmids

Plasmid pGPMRns-Myc is a derivative of pTags2 (Addgene) that expresses Rns-myc from *lacp. rns* was amplified from pGPMRns (Maria Del Rocio Bodero *et al.*, 2007) with primers 1519/1522. pTags2 vector backbone was amplified with primers 1414/1419. The two PCR products were Dpn1 digested then circularized with NEB HiFi. Site-directed mutagenesis on pGPMRns-Myc with primers 1565/1566 and 1567/1568 followed by NEB HiFi assembly resulted in plasmids pGPMRnsH20A and pGPMRnsR75A respectively. Sanger sequencing was used to confirm mutagenesis.

Reporter strains

Plasmid pHKLac1 is a promotorless *lacZ* reporter integration plasmid with a *pir*-dependent origin of replication (Haldimann and Wanner, 2001). It carries $attP_{HK022}$ for Int_{HK022}-mediated integration into the chromosome of *E. coli* at $attB_{HK022}$. The *cs3* intergenic region (-121 to +352 relative to *cs3* ORF) was amplified from ETEC strain 1392-75-2a with primers CS3-for and CS3-rev. The *nlpA-yicS* intergenic region was amplified from ETEC strain H10407 with primers nlpA-F1 and nlpA-r1(Maria Del Rocio Bodero *et al.*, 2007). The PCR products were digested with BamHI and EcoRI and then ligated into the same sites of pHKLac1 to construct pCS3Lac1 [*cs3p*(-121 to +352)*::lacZ*] and pNlpALac1 [*nlpAp*(-391 to +58*)::lacZ*]. Each reporter plasmid was then integrated into the chromosome of MC4100 *[F- araD139 Δ(argF-lac)U169 rpsL150* (StrR*) relA1 flhD5301 deoC1 ptsF25 rbsR]* (Casadaban, 1976) as previously described (Haldimann and Wanner, 2001) resulting in strains GPM1072 ($attB_{HK022}$::pCS3Lac1) and GPM1080 ($attB_{HK022}$::pNlpALac1). Colony PCR was used to verify that each strain possessed only a single plasmid integrant, as previously described (Haldimann and Wanner, 2001).

B-galactosidase assays

Lac reporter strains GPM1072 and GPM1080 were transformed with pGPMRns-Myc, pGPMRnsH20A, pGPMRnsR75A, or vector pTags2 to determine the effect of decanoic acid on the ability of Rns to regulate Rns-dependent promoters. All strains were grown aerobically at 37C to stationary phase in LB medium with 100μg/mL ampicillin with or without decanoic acid in 0.4% vol/vol DMSO. B-galactosidase activity was assayed as previously described (Miller, 1972).

Immunoblots

ETEC strains H10407 and 1392/75-2a were grown to stationary phase in CFA (Evans *et al.*, 1977) medium with or without decanoic acid in 0.4% vol/vol DMSO. Pilins were released from the outer membrane by incubating ETEC in 1/10 volume PBS at 65C for 20 minutes. Supernatants were clarified by centrifugation to remove insoluble material.

Stationary phase whole cell lysates of ETEC, DH5α strains expressing Rns-Myc and derivatives, or 10 *μ*g pilin supernatants were subjected to SDS-PAGE, transferred to PVDF membranes, and blocked in TBS-Blotto (25 mM TrisCl pH 7.6, 150 mM NaCl, 5% wt/vol powdered nonfat milk. Antibodies against CexEα (H10407) and CexEε (1392/75-2a) were produced by immunization of rabbits (Proteintech Group, Inc.) with purified antigens and used at a dilution of 1:5,000 in TBS-Blotto with 0.05% vol/vol Tween20 (Pilonieta *et al.*, 2007; Rivas *et al.*, 2020) Primary antibodies against c-Myc (Sigma-Aldrich M4439) and DnaK (AbCam ab69617) were used at dilutions of 1:5,000 and 1:10,000 respectively. HRP conjugated goat anti-rabbit (Santa Cruz Biotechnology sc-2030) and goat anti-mouse (Jackson ImmunoResearch 115-036-062) antibodies were used at 1:10,000 dilutions. Chemiluminescence was detected with an Odyssey FC Imaging System (LI-COR Biosciences).

Results

Identification of proteins potentially regulated by UFAs

Secondary structure prediction and alignments identified eight AraC proteins that are known virulence regulators and that we predict may be regulated by UFAs (Fig 1, Table 1). Many of these proteins did not contain a lysine in the area corresponding to Lys230 in ToxT, but rather an arginine, and in one case histidine. When these proteins were compared to an existing phylogenic tree of fifty-eight AraC family proteins (Ibarra *et al.*, 2008), all were found to be among the most closely related to ToxT. This supports our hypothesis that these AraC family members could share a common mechanism of being regulated by fatty acid ligands and served as a foundation for subsequent structural and functional analysis of these target proteins.

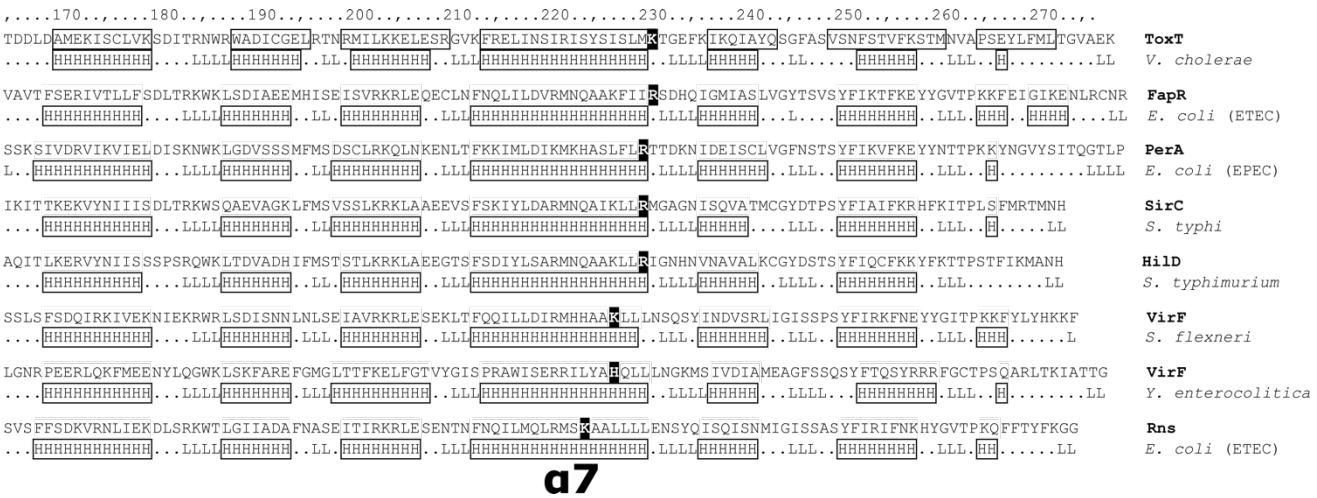

Figure 1: *Structural alignment of the C-terminal domains of the top AraC family hits*. ToxT is shown at the top with structurally determined α-helices shown in boxes. For the other proteins, H indicates predicted α-helices and L indicates predicted loop regions. The position of α7 is indicated and the positive residues are highlighted for each sequence. Predictions by the PROF algorithm using the server at http://predictprotein.org.

Initial structure determination

As we pursued several of these targets for biochemical and structural studies, we were able to crystallize and obtain diffraction data for Rns. As attempts at molecular replacement using ToxT and other AraC family member structures as phasing models were unsuccessful, we used SeMet labeling coupled with single-wavelength anomalous dispersion (SAD) to experimentally determine phases and solve the structure. As expected, Rns shows the hallmarks of AraC proteins, with a cupin-like N-terminal domain and helix-turn-helix containing DNA binding domain (DBD) (Fig 2A). The N-terminal domain (residues 1-158) contained 6 β-strands and 4 α-helices. The fourth helix is connected through a three residue linker to the DBD. The DNA binding domain (residues 162-265) is typical for this family of proteins, consisting of seven alpha helices. Interestingly, one monomer was found to be in an open conformation in which the N- and C-terminal domains were separated, forming a groove containing electron density consistent with a bound ligand. In addition, the protein formed a dimer across a crystal contact in the N-terminal domain similar to other AraC proteins that are known to dimerize (Soisson *et al.*, 1997; Shrestha *et al.*, 2015).

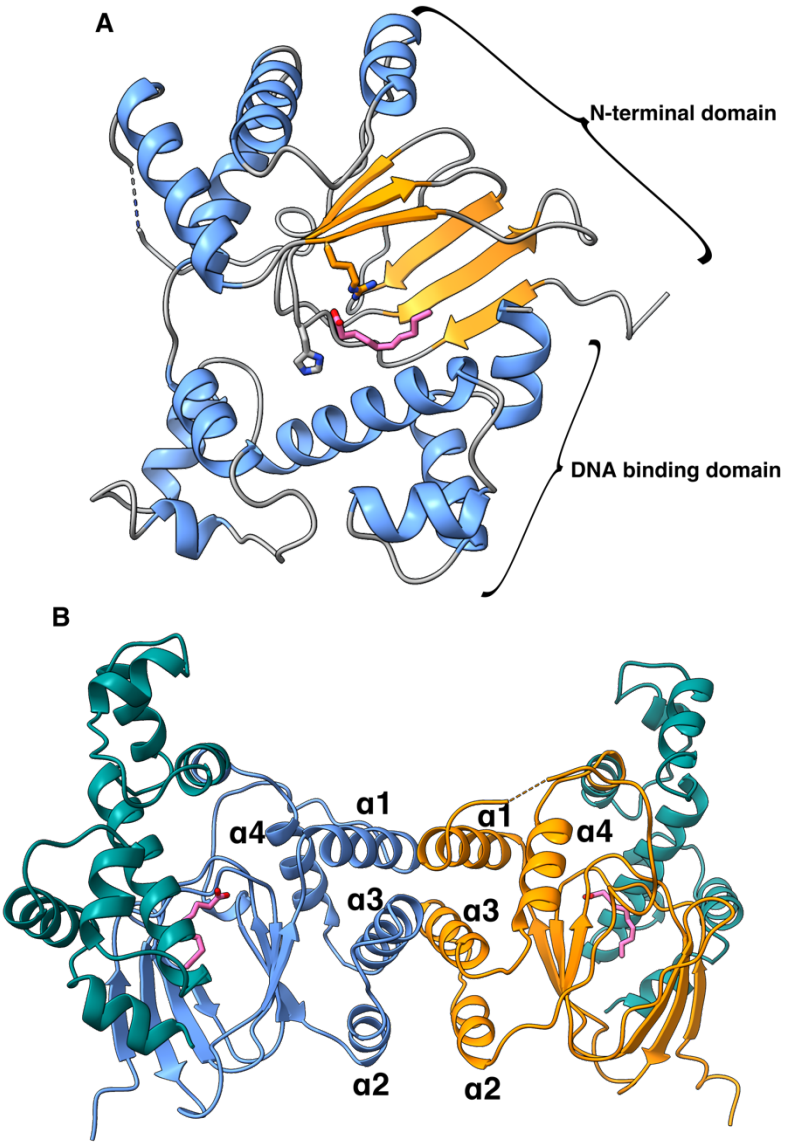

Figure 2: *Structure of Rns and the potential dimerization interface.* **A**. Structure of SeMet-Rns showing decanoic acid modeled in the ligand binding pocket with α-helices in blue, β-sheets in orange, coils in gray, and the decanoic acid in pink. The N-terminal and DNA binding domains are labeled. **B**. Proposed biological dimer with the N-terminal domains of the two monomers in orange or blue and both DNA binding domains in teal. The N-terminal α-helices are labeled.

Rns has a dimer interface

Rns formed a dimer across a crystallographic symmetry axis with helices α1-α3 from the N-terminal domain forming an interface consistent with physiological function (Fig 2B). The helices from the two monomers face each other in an antiparallel fashion in a manner similar to ExsA, another AraC family member from *Pseudomonas aeruginosa* involved in the transcription of the type three secretion system (Frank and Iglewski, 1991; Shrestha *et al.*, 2015). In Rns, much of the interface is between α1 and α3, burying approximately 274 $Å^2$ of surface area. The interface forms in such a way that the DNA binding domains of the two Rns monomers are pointing almost 180° away from each other (Fig 2B), implying Rns is capable of binding looped DNA in a manner similar to AraC (Lobell and Schleif, 1990). Ongoing studies in our

laboratories are focused on investigating the relevance of the dimerization interface.

Rns contains an unexpected ligand

Analysis of the crystal structure revealed unexpected electron density in the groove between the N- and C-terminal domains consistent with the presence of a medium chain fatty acid. Initially, octanoic acid, an eight-carbon fatty acid was added to the model. While this improved the R factor, the density appeared to be able to accommodate a larger molecule. When decanoic acid was modeled, the refinement statistics improved, and the two additional carbons filled the remaining electron density (Fig 3A). As no exogenous fatty acids were added to Rns during purification or crystallization, the presence of bound fatty acid in the structure suggested a possible physiological role, and therefore we proceeded with functional analysis of the effect of fatty acids on Rns activity.

Decanoic acid binds to Rns and inhibits its activity

Differential scanning fluorometry (DSF) was used to determine if decanoic acid and other fatty acids could interact with Rns. DSF experiments were performed with decanoic acid (10 carbons), octanoic acid (8 carbons), and palmitic acid (16 carbons). While octanoic acid did not change the melting temperature (T_m) of Rns, palmitic acid decreased its T_m and

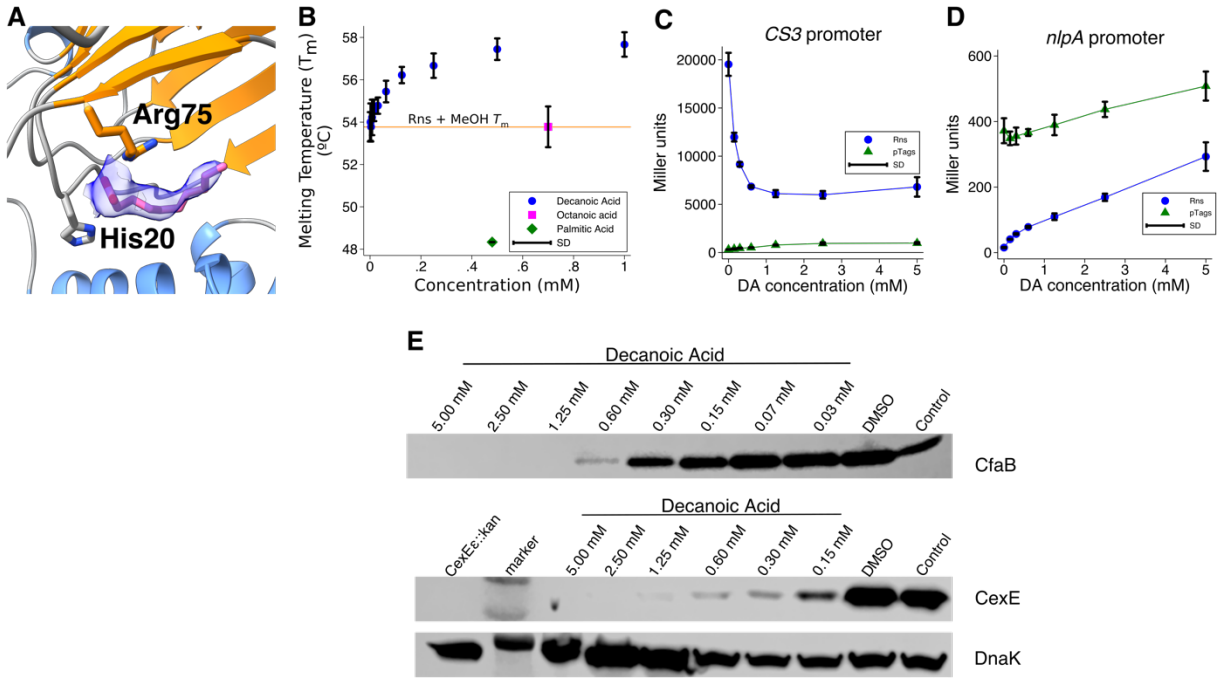

Figure 3: *Rns binds decanoic acid, which influences Rns activity.* **A**. Detail showing the electron density from an 2Fo-Fc omit map contoured to 1σ around the decanoic acid as a blue volume. **B.** DSF showing an increase in the T_m of Rns in a dose dependent manner with decanoic acid. Octanoic acid does not affect the T_m of Rns and palmitic acid decreases the melting temperature of Rns. Data is shown as the mean ± SD, n=3. **C**. B-galactosidase assays showing decanoic acid represses Rns activity at the CS3 promoter and **D**. causes Rns derepression at the nlpA promoter. Data is given as the mean response ± SD, n=3. **E.** Western blots of CfaB (top) and CexE (lower) showing decreased expression when increasing concentrations of decanoic acid were added to the culture.

decanoic acid increased the T_m in a dose dependent manner up to a concentration of 1 mM (Fig 3B). This is consistent with decanoic acid interacting specifically with Rns.

As the DSF showed decanoic acid interacts with Rns, we evaluated its effect at Rns

activated (*CS3p*) and repressed (*nlpAp*) promoters using Lac reporter strains (Favre *et al.*, 2006; Maria Del Rocio Bodero *et al.*, 2007). Consistent with the structure and DSF results, addition of exogenous decanoic acid inhibited Rns-dependent expression of β-galactosidase from *CS3p* in a dose-dependent manner (Fig 3C). Inhibition was not the result of nonspecific interactions, as exogenous decanoic acid also relieved Rns-dependent repression of the *nlpAp*, mirroring the effects at the *CS3p* (Fig 3D). As both repression and activation require Rns binding at sites near each promoter ((Maria Del Rocio Bodero *et al.*, 2007), and Munson, unpublished), these results suggest decanoic acid directly interferes with the ability of Rns to bind DNA.

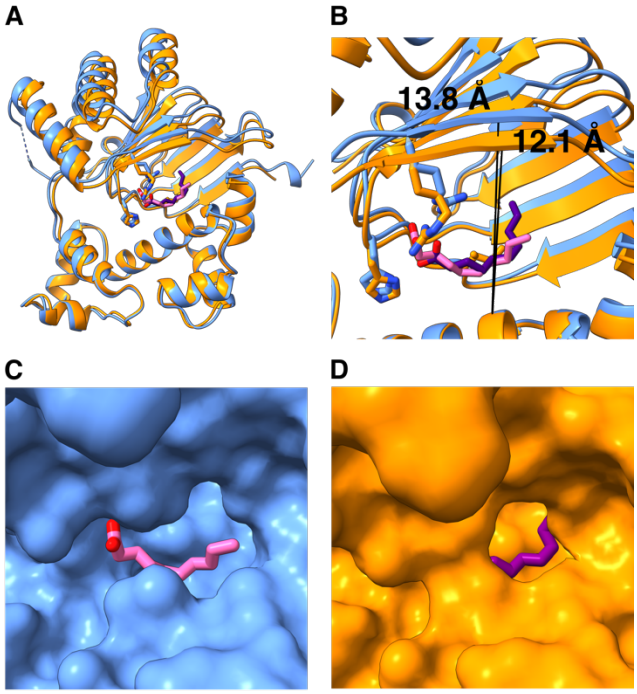

Figure 4: *Comparison of the SeMet labeled structure in the open conformation and the native Rns structure in the closed conformation.* **A.** Superposition of the native (orange) and SeMet Rns (blue) structures, the two domains were aligned using the long helix in the DNA binding domain (Phe205-Glu223), showing how the N-terminal domain is shifted away from the DBD in the SeMet structure. **B**. Detail showing the β-sheet Is shifted by ~2 Å from the DBD in the SeMet structure compared to the native structure. **C.** Surface representation of the SeMet-Rns structure in blue with the decanoic acid in pink showing how the fatty acid is exposed to solvent. **D.** Surface representation of the native Rns in orange with the decanoic acid in purple showing how the ligand is enclosed in more of a pocket.

To determine if decanoic acid can inhibit in situ virulence gene expression, the fatty acid was added to ETEC cultures. Consistent with the results from K-12 Lac reporter strains, we found that increasing concentrations of decanoic acid inhibited the expression of the CFA/I major pilin CfaB in ETEC H10407 (Fig 3E top panel). This was not limited to H10407 because the expression of CexEε from ETEC strain 1392/75-2a was also inhibited by the presence of decanoic acid (Fig 3E middle panel). The apparent lack of an effect upon DnaK suggest decanoic acid specifically inhibits the Rns regulon (Fig 3E bottom panel). Thus, exogenous decanoic acid abolishes the expression of ETEC virulence factors by inhibiting the activity of the Rns transcription factor. This is the first evidence of a small molecule inhibitor of ETEC virulence and has significant implications for therapeutic applications.

Structure with decanoic acid

Given decanoic acid both stabilized and affected Rns function, Rns was crystalized in the presence of excess decanoic acid to assess what effects this might have on its structure. Despite the diffraction data showing significant pseudo-translation, the structure was solved to 3.0 Å using molecular replacement with the apo SeMet-Rns structure as a search model. Analysis of the resulting electron density showed both monomers contained a ligand, and decanoic acid was placed in the density.

Overall, the SeMet and the unlabeled Rns structures are quite similar. Interestingly, in the unlabeled structure both monomers were in a closed conformation. Therefore, we examined differences between the open monomer observed in the SeMet structure and a

closed monomer of the unlabeled structure. In the SeMet structure, the ligand binding groove is open as a result of helices making up the dimer interface and β-strands 2, 4, and 6 shifting away from the long helix in the DBD by ~1.7 Å in comparison to the native Rns structure (Fig 4A and B). This shift results in the binding pocket closing in around decanoic acid (compare Fig 4C to 4D).

Arg75 and His20 in the structures make contact with the decanoic acid

Both the open and closed conformations show His20 and Arg75 interacting with the carboxyl group of the decanoic acid (Fig 5A and 5B). We note that Lys216, which was the positively charged residue identified by our computational screen as potentially interacting with the fatty acid (Fig. 1), does not interact with the ligand. Interestingly, in the open structure Arg75 is between the fatty acid and the rest of the N-terminal domain (Fig5A right panel), compared to the closed Rns where Arg75 is more alongside the ligand (Fig 5A left panel). In addition, the position of the decanoic acid head group is in a different orientation in the open and closed conformations. In the open conformer the head group is perpendicular to the plane of the imidazole group of His20 resulting in only one oxygen from the fatty acid making contacts with His20 and Arg75 (Fig5A and B right panel). In the closed conformation the fatty acid carboxyl group is turned 90º allowing both oxygens to make contacts with either His20 and Arg75 (Fig 5A and B left panel). It is interesting to speculate that the position of the Arg75 drives the transition between open and closed conformations. The role of Arg75 and His20 in mediating the structural response of Rns binding to decanoic acid is being explored.

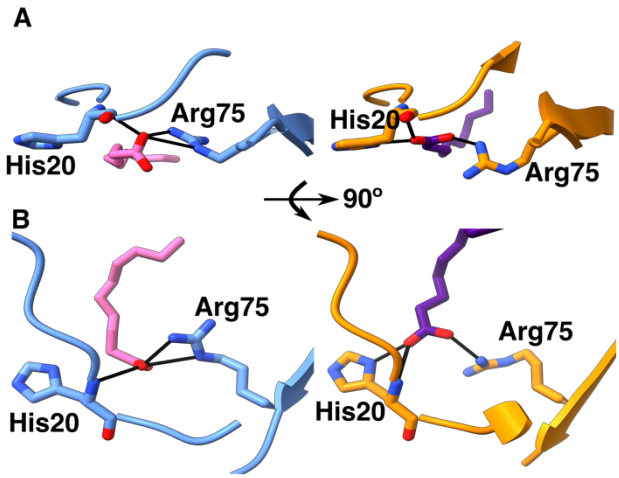

Figure 5: *Detail showing the interactions between His20 and Arg75 to decanoic acid.* **A.** "front" view showing how the Arg75 in the SeMet-Rns, in blue, is above the decanoic acid (right panel) while in the native-Rns, in orange, Arg75 (left panel) is alongside the fatty acid. **B**. "Top" view with the SeMet-Rns in blue (right panel) and native-Rns in orange (left panel).

Comparison of Rns and ToxT binding pockets

Given Rns and ToxT are the only full-length AraC structures solved with bound fatty acids it is interesting to compare the fatty acid binding mode of the two proteins. Based on crystal structures, the proteins bind fatty acids of different lengths and degree of saturation: palmitoleate (16 carbon monounsaturated) binds to ToxT, while decanoate (10 carbon saturated) binds to Rns. To compare the ToxT structure (3GBG) (Lowden *et al.*, 2010) to the native Rns structure, residues 211-231 from ToxT were aligned with residues 205-223 from Rns in Chimerax (Goddard *et al.*, 2017). While both fatty acids are bound between the N-terminal domain and the DBD (Fig 6), in ToxT the bound fatty acid projects more deeply into

the N-terminal domain (compare Fig 6A to 6B). Interestingly, in ToxT residues from the N-terminal domain (Lys31) and the DBD (Lys230) interact with carboxyl group on the fatty acid (Fig 6A), while in Rns the two residues that interact with the carboxyl group are in the N-terminal domain (Fig 6B). Furthermore, the β1-strand in ToxT is absent in the Rns structure (compare Fig 6A to 6B), creating a more enclosed pocket in ToxT (Fig 6C), whereas Rns has an opening in the side of the pocket (Fig 6D). Both pockets are hydrophobic except for the charged groups involved in binding the carboxyl portion of the fatty acid (Fig 6C and 6D). In addition, palmitoleate occupies a larger portion of the binding pocket in ToxT than the decanoate does in Rns (Fig 6C and 6D), suggesting Rns is able to bind to fatty acid ligands larger than decanoate. It is interesting to note while fatty acids regulate both proteins, the details of the binding are different and this is likely to be a theme across fatty acid regulated AraC's.

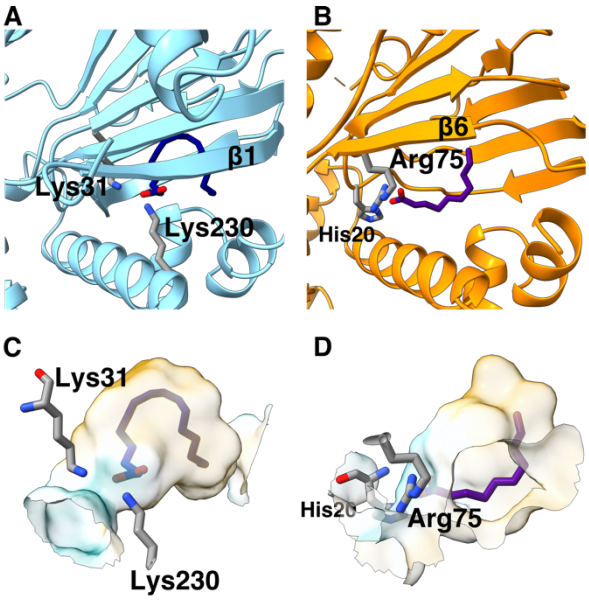

Figure 6: *Comparison of the binding pockets of ToxT and Rns.* **A.** ToxT in blue with the palmitoleic acid in dark blue. **B.** The native Rns in orange with the decanoic acid in purple were aligned in Chimerax (Goddard *et al.*, 2017) using the long helix in the DBD. The β-strand for each protein closest to the long helix in the DBD are labeled, as well as the residues which make contacts with the fatty acids. The binding pockets for **C.** ToxT and **D.** Rns are shown. The surfaces are colored according to lipophilicity calculated using Chimerax (Goddard *et al.*, 2017), with cyan for charged areas and orange for hydrophobic surfaces. Again, the residues interacting with fatty acids are labeled.

Discussion

As part of ongoing efforts to determine whether other AraC proteins are regulated by fatty acids in a similar fashion as ToxT, we solved the structure of Rns using X-ray crystallography in two conformations: open, distinguished by having a groove between the N and C-terminal domains for ligand binding; and closed, where the two domains have come closer together with the pocket enclosing the ligand. In addition, the Rns structures were dimeric, with an interface similar to structures of other AraC proteins (Soisson *et al.*, 1997; Shrestha *et al.*, 2015). The DNA binding domains of the two monomers are pointing 180º apart from each other, suggesting Rns binds to DNA loops in a manner similar to AraC (Lobell and Schleif, 1990), and consistent with the observation that most Rns regulated promoters have a proximal site and a distal site separated by about forty base pairs, although at some promoters this is less and at others the sites are separated by over a hundred base pairs (Munson and Scott, 1999; Munson and Scott, 2000; Maria Del Rocio Bodero *et al.*, 2007; Pilonieta *et al.*, 2007; Maria Del Tocio Bodero *et al.*, 2008; Maria Del Rocio Bodero and Munson, 2016). For instance, *CS1* pili expression is mediated by two sites, one proximal to the -35 RNAP binding site, and one distal, around -106, to the transcription start site (Munson and Scott, 1999). The sites are asymmetric and contribute additively to the expression of the *CS1* pili. Another example is the *rns* promoter has two Rns binding sites required for transcription, one at the -227 position and the other downstream of the transcription start site (Munson and Scott, 2000). In this instance the binding sites are widely spaced and act synergistically as both binding sites are required for activating transcription (Munson and Scott, 2000). These findings, coupled with the

observations from our structures, indicate Rns likely binds to looped DNA. Work is ongoing to investigate the relevance of this interface and to clarify if Rns binds looped DNA.

Importantly, the ligand binding pocket of Rns was occupied by the 10-carbon fatty acid, decanoic acid. DSF studies showed decanoic acid specifically stabilized Rns, as octanoic and palmitic acids did not. Decanoic acid also influenced Rns activity at the *CS3* promoter, where Rns activates transcription, and at the *nlpA* promoter, where Rns represses transcription (Maria Del Rocio Bodero *et al.*, 2007; Maria Del Tocio Bodero *et al.*, 2008). In addition, decanoic acid was able to repress the expression of Rns regulated CexE and the CFA/I pilin in ETEC strains. Furthermore, structural analysis has identified possible residues involved in binding to decanoic acid. Therefore, we have identified a small molecule that inhibits ETEC virulence expression.

While the specific structural mechanism by which Rns is regulated by decanoic acid is not clear, the mechanism by which fatty acid inhibition occurs is likely linked to influencing the stability of the Rns dimer, either directly or by a dynamic allosteric mechanism as demonstrated for *V. cholerae* ToxT (Cruite *et al.*, 2019). Future studies will be directed at clarifying this mechanism. The inhibition of Rns by a fatty acid represents the first time a small molecule has been shown to bind to Rns and inhibit virulence gene expression in ETEC. Decanoic acid and its analogs should be pursued as lead anti-virulence compounds, as they could be viable alternatives to decades of failed strategies to develop an effective vaccine against ETEC.

Data Availability: The structures of Rns have been deposited into the PDB: SeMet-Rns; 6XIV, and Rns; 6XIU.

Acknowledgments: Research reported in this publication was supported by the NIAID of the National Institutes of Health under award number AI128164 (GPM) as well as AI072661 and AI140740 (FJK). Additional support was provided by BioMT COBRE P20-GM113132. Sequencing was performed by the Molecular Biology Shared Resource at Dartmouth. This research used the FMX and AMX beamlines of the National Synchrotron Light Source II, a U.S. Department of Energy (DOE) Office of Science User Facility operated for the DOE Office of Science by Brookhaven National Laboratory under Contract No. DE-SC0012704. The Life Science Biomedical Technology Research resource is primarily supported by the National Institute of Health, National Institute of General Medical Sciences (NIGMS) through a Center Core P30 Grant (P30GM133893), and by the DOE Office of Biological and Environmental Research (KP1605010). We also acknowledge the beam line staff at NSLS2-FMX and AMX for making data collection possible. The contents of this publication are solely the responsibility of the authors and do not necessarily represent the official views of the National Institutes of Health.

References:

Adams, P.D., Afonine, P.V., Bunkoczi, G., Chen, V.B., Davis, I.W., Echols, N., *et al.* (2010) PHENIX: a comprehensive python-based system for macromolecular structure solution. *Acta Crystallogr D Biol Crystallogr* **66**: 1–9.

Bodero, M.D.R., and Munson, G.P. (2016) The virulence regulator Rns activates the expression of CS14 pili. *Genes (Basel)* **7**.

Bodero, M.D.R., Pilonieta, M.C., and Munson, G.P. (2007) Repression of the Inner Membrane Lipoprotein NlpA by Rns in Enterotoxigenic Escherichia coli. *Journal of Bacteriology* **189**: 1627–1632.

Bodero, M.D.T., Harden, E.A., and Munson, G.P. (2008) Transcriptional regulation of subclass 5b fimbriae. *BMC Microbiol* **8**: 180–10.

Boedeker, E.C. (2005) Vaccines for enterotoxigenic *Escherichia coli*: current status. *Curr Opin Gastroenterol* **21**: 15–19.

Caron, J., Coffield, L.M., and Scott, J.R. (1989) A plasmid-encoded regulatory gene, *rns*, required for expression of the CS1 and CS2 adhesins of enterotoxigenic *Escherichia coli*. *Proceedings of the National Academy of Sciences* **86**: 963–967.

Caron, J., Maneval, D.R., Kaper, J.B., and Scott, J.R. (1990) Association of *rns* homologs with colonization factor antigens in clinical *Escherichia coli* isolates. *Infection and Immunity* **58**: 3442–3444.

Casadaban, M.J. (1976) Transposition and fusion of the *lac* genes to selected promoters in *Escherichia coli* using bacteriophage lambda and Mu. *J Mol Biol* **104**: 541–555.

Chatterjee, A., Dutta, P.K., and Chowdhury, R. (2007) Effect of fatty acids and cholesterol present in bile on expression of virulence factors and motility of *Vibrio cholerae*. *Infection and Immunity* **75**: 1946–1953.

Cruite, J.T., Kovacikova, G., Clark, K.A., Woodbrey, A.K., Skorupski, K., and Kull, F.J. (2019) Structural basis for virulence regulation in Vibrio cholerae by unsaturated fatty acid components of bile. *Communications Biology* **2**: 440–9.

DiRita, V.J., Parsot, C., Jander, G., and Mekalanos, J.J. (1991) Regulatory cascade controls virulence in *Vibrio cholerae*. *Proceedings of the National Academy of Sciences* **88**: 5403–5407.

Emsley, P., and Cowtan, K. (2004) Coot: model-building tools for molecular graphics. *Acta Crystallogr D Biol Crystallogr* **60**: 2126–2132.

Evans, D.G., Evans, D.J., and Tjoa, W. (1977) Hemagglutination of human group a erythrocytes by enterotoxigenic *Escherichia coli* isolated from adults with diarrhea: correlation with colonization factor. *Infection and Immunity* **18**: 330–337.

Favre, D., Lüdi, S., Stoffel, M., Frey, J., Horn, M.P., Dietrich, G., *et al.* (2006) Expression of enterotoxigenic Escherichia coli colonization factors in Vibrio cholerae. *Vaccine* **24**: 4354–4368.

Fleckenstein, J.M., and Kuhlmann, F.M. (2019) Enterotoxigenic *Escherichia* coli Infections. *Curr Infect Dis Rep* **21**: 9–9.

Frank, D.W., and Iglewski, B.H. (1991) Cloning and sequence analysis of a trans-regulatory locus required for exoenzyme S synthesis in *Pseudomonas aeruginosa*. *Journal of Bacteriology* **173**: 6460–6468.

Gallegos, M.-T., Schleif, R., Bairoch, A., Hofmann, K., and Ramos, J.L. (1997) Arac/XylS family of transcriptional regulators. *Microbiol Mol Biol Rev* **61**: 393–410.

Goddard, T.D., Huang, C.C., Meng, E.C., Pettersen, E.F., Couch, G.S., Morris, J.H., and Ferrin, T.E. (2017) UCSF ChimeraX: meeting modern challenges in visualization and analysis. *Protein Science* **27**: 14–25.

Haldimann, A., and Wanner, B.L. (2001) Conditional-replication, integration, excision, and retrieval plasmid-host systems for gene structure-function studies of bacteria. *Journal of Bacteriology* **183**: 6384–6393.

Higgins, D.E., Nazareno, E., and DiRita, V.J. (1992) The virulence gene activator ToxT from *Vibrio cholerae* is a member of the AraC family of transcriptional activators. *Journal of Bacteriology* **174**: 6974–6980.

Ibarra, J.A., Perez-Rueda, E., Segovia, L., and Puente, J.L. (2008) The DNA-binding domain as a functional indicator: the case of the AraC/XylS family of transcription factors. *Genetica* **133**: 65–76.

Jiang, Z.D., and DuPont, H.L. (2017) Etiology of travellers' diarrhea. *J Travel Med* **24**: S13–S16.

Kabsch, W. (2010) XDS. *Acta Crystallogr D Biol Crystallogr* **66**: 1–8.

Khalil, I.A., Troeger, C., Blacker, B.F., Rao, P.C., Brown, A., Atherly, D.E., *et al.* (2018) Morbidity and mortality due to shigella and enterotoxigenic *Escherichia coli* diarrhoea: the Global Burden of Disease Study 1990-2016. *Lancet Infect Dis* **18**: 1229–1240.

LaRonde-LeBlanc, N., and Wolberger, C. (2000) Characterization of the oligomeric states of wild type and mutant AraC. *Biochemistry* **39**: 11593–11601.

Lobell, R.B., and Schleif, R.F. (1990) DNA looping and unlooping by AraC protein. *Science* **250**: 528–532.

Lowden, M.J., Skorupski, K., Pellegrini, M., Chiorazzo, M.G., Taylor, R.K., and Kull, F.J. (2010) Structure of Vibrio cholerae ToxT reveals a mechanism for fatty acid regulation of virulence genes. *Proc Natl Acad Sci USA* **107**: 2860–2865.

Mahon, V., Smyth, C.J., and Smith, S.G.J. (2010) Mutagenesis of the Rns regulator of enterotoxigenic Escherichia coli reveals roles for a linker sequence and two helix-turn-helix motifs. *Microbiology* **156**: 2796–2806.

McCoy, A.J., Grosse-Kunstleve, R.W., Adams, P.D., Winn, M.D., Storoni, L.C., and Read, R.J. (2007) Phaser crystallographic software. *J Appl Cryst* **40**: 1–17.

Midgett, C.R., Almagro-Moreno, S., Pellegrini, M., Taylor, R.K., Skorupski, K., and Kull, F.J. (2017) Bile salts and alkaline pH reciprocally modulate the interaction between the periplasmic domains of *Vibrio cholerae* ToxR and ToxS. *Molecular Microbiology* **105**: 258–272.

Miller, J.H. (1972) *Experiments in Molecular Genetics*. Cold Spring Harbor Laboratory Press, Cold Spring Harbor, NY.

Munson, G.P. (2013) Virulence regulons of enterotoxigenic *Escherichia coli*. *Immunol Res* **57**: 229–236.

Munson, G.P., and Scott, J.R. (1999) Binding site recognition by Rns, a virulence regulator in the AraC family. *Journal of Bacteriology* **181**: 2110–2117.

Munson, G.P., and Scott, J.R. (2000) Rns, a virulence regulator within the AraC family, requires binding sites upstream and downstream of its own promoter to function as an activator. *Molecular Microbiology* **36**: 1391–1402.

Niesen, F.H., Berglund, H., and Vedadi, M. (2007) The use of differential scanning fluorimetry to detect ligand interactions that promote protein stability. *Nat Protoc* **2**: 2212–2221.

Pettersen, E.F., Goddard, T.D., Huang, C.C., Couch, G.S., Greenblatt, D.M., Meng, E.C., and Ferrin, T.E. (2004) UCSF Chimera--a visualization system for exploratory research and analysis. *J Comp Biol* **25**: 1605–1612.

Pilonieta, M.C., Bodero, M.D.T., and Munson, G.P. (2007) CfaD-dependent expression of a novel extracytoplasmic protein from Enterotoxigenic *Escherichia coli*. *Journal of Bacteriology* **189**: 5060–5067.

Porter, C.K., Olson, S., Hall, A., and Riddle, M.S. (2017) Travelers' Diarrhea: An Update on the Incidence, Etiology, and Risk in Military Deployments and Similar Travel Populations. *Military Medicine* **182**: 4–10.

Rivas, Z.P., Talbot, K.M., Merselis, L.C., McCormack, R.M., Adkins, B., and Munson, G.P. (2020) CexE Is a coat protein and virulence factor of diarrheagenic pathogens. *Front Microbiol* **11**: 1374.

Shakoor, S., Platts-Mills, J.A., and Hasan, R. (2019) Antibiotic-Resistant Enteric Infections. *Infect Dis Clin North Am* **33**: 1105–1123.

Shrestha, M., Xiao, Y., Robinson, H., and Schubot, F.D. (2015) Structural analysis of the regulatory domain of ExsA, a key transcriptional regulator of the type three secretion system in *Pseudomonas aeruginosa*. *PLoS ONE* **10**: e0136533–17.

Soisson, S.M., MacDougall-Shackleton, B., Schleif, R., and Wolberger, C. (1997) Structural basis for ligand-regulated oligomerization of AraC. *Science* **276**: 421–425.

Studier, F.W. (2005) Protein production by auto-induction in high-density shaking cultures. *Protein Expr Purif* **41**: 207–234.

Troeger, C., Forouzanfar, M., Rao, P.C., Khalil, I., Brown, A., Reiner, R.C., Jr, *et al.* (2017) Estimates of global, regional, and national morbidity, mortality, and aetiologies of diarrhoeal diseases: a systematic analysis for the Global Burden of Disease Study 2015. *Lancet Infect Dis* **17**: 909–948.

Turner, S.M., Scott-Tucker, A., Cooper, L.M., and Henderson, I.R. (2006) Weapons of mass destruction: virulence factors of the global killer enterotoxigenic *Escherichia coli*. *FEMS Microbiology Letters* **263**: 10–20.

Vidal, R.M., Muhsen, K., Tennant, S.M., Svennerholm, A.-M., Sow, S.O., Sur, D., *et al.* (2019) Colonization factors among enterotoxigenic *Escherichia coli* isolates from children with moderate-to-severe diarrhea and from matched controls in the Global Enteric Multicenter Study (GEMS). *PLoS Negl Trop Dis* **13**: e0007037–27.

World Health Organization (1999) New frontiers in the development of vaccines against enterotoxinogenic (ETEC) and enterohaemorrhagic (EHEC) *E. coli* infections. Part I. *Wkly Epidemiol Rec* **74**: 98–101.

Table 1: List of potential ToxT like AraC proteins			
Protein	**Organism**	**UniProt ID**	**Criteria met**
FapR	*E. coli* – ETEC	P23774	1-4
PerA	*E. coli* – EPEC	P43459	1-4
SirC	*S. typhi*	Q8Z4A6	1-4
HilD	S. *typhimurium*	P0CL08	1-4
VirF	*S. flexneri*	P0A2T1	1, 2, 4
VirF	*Y. enterocolitica*	P0C2V5	1, 2, 4
Rns	*E. coli* – ETEC	P16114	1, 2, 4

Table 2: Refinement Statistics		
	SeMet-Rns	**Rns**
Wavelength		
Resolution range	29.29 - 2.8 (2.9 - 2.8)	27.39 - 3.0 (3.107 - 3.0)
Space group	P 21	P 21 21 21
Unit cell	72.51 49.97 102.92 90 106.11 90	48.24 95.15 133.09 90 90 90
Total reflections	228834 (24784)	81535 (8041)
Unique reflections	17538 (1743)	12798 (1219)
Multiplicity	13.0 (14.2)	6.4 (6.6)
Completeness (%)	94.93 (86.50)	99.16 (97.50)
Mean I/sigma(I)	8.67 (0.74)	7.29 (0.88)
Wilson B-factor	89.24	93.97
R-merge	0.1984 (3.508)	0.1518 (1.994)
R-meas	0.2069 (3.637)	0.1654 (2.162)
R-pim	0.0579 (0.956)	0.06498 (0.8261)
CC1/2	0.995 (0.29)	0.997 (0.549)
CC*	0.999 (0.671)	0.999 (0.842)
Reflections used in refinement	16917 (1532)	12745 (1211)
Reflections used for R-free	1679 (143)	1277 (120)
R-work	0.2422 (0.3928)	0.2571 (0.3840)
R-free	0.2999 (0.4694)	0.3007 (0.4249)
CC(work)	0.948 (0.589)	0.955 (0.646)
CC(free)	0.911 (0.461)	0.915 (0.423)
Number of non-hydrogen atoms	4222	4068
macromolecules	4189	4044
ligands	33	24

Protein residues	513	494
RMS(bonds)	0.008	0.012
RMS(angles)	1.17	1.36
Ramachandran favored (%)	93.89	92.39
Ramachandran allowed (%)	5.92	7.2
Ramachandran outliers (%)	0.2	0.41
Rotamer outliers (%)	4.99	6.9
Clashscore	7.4	19.06
Average B-factor	93.97	83.91
macromolecules	94.01	84.04
ligands	89.13	61.91

Table 3
Strains used in this study

Strain	Characteristics	Source
MC4100	*F- araD139 Δ(argF-lac)U169 rpsL150* (StrR*) relA1 flhD5301 deoC1 ptsF25 rbsR*	(Haldimann & Wanner 2001)
GPM1072	MC4100 *attB*$_{HK022}$:☹pCS3Lac1*; attP*$_{HK022}$ *aadA rrnB Pcs3 lacZYA tL3*)	This study
GPM1080	MC4100 *attB*$_{HK022}$:☹pNlpALac1*; attP*$_{HK022}$ *aadA rrnB Pcs3 lacZYA tL3*)	(Bodero, Pilonieta, and Munson 2007)
H10407	ETEC O78::H11:K80 CFA/I+ ST+ LT+	(Crossman et al. 2010)
1392/75-2a	ETEC O6:H16:K15 CS31+ CS3+ ST+ LT+	(Crossman et al. 2010)

Table 4 **Plasmids used in this study**			
Name	**Description**	**Marker**	**Source**
pTags2	Cloning vector	Amp	Addgene
pGPMRns	Rns expressed from *lacp*	Amp	(Bodero, Pilonieta, and Munson 2007)
pGPMRns-Myc	Rns-Myc expressed from *lacp*	Amp	This study
pGPMRnsH20A	RnsH20A-Myc expressed from *lacp*	Amp	This study
pGPMRnsR75A	RnsR75A-Myc expressed from *lacp*	Amp	This study
pHKLac1	Integration plasmid	aadA	(Haldimann and Wanner 2001)
pCS3Lac1	Integration plasmid [*cs3p*(-121 to +352)*::lacZ*]	aadA	This study
pNlpALac1	Integration plasmid [*nlpAp*(-391 to +58*)::lacZ*].	aadA	(Bodero, Pilonieta, and Munson 2007)

Table 5 **Oligonucleotides used in this study**	
Name	**Sequence**
1414	CATATGTATATCTCCTTCTTTGGCC
1419	GAACAGAAACTGATTAGCGAAG
1519	gccaaagaaggagatatacatATGGACTTTAAATACACTGAAG

1522	cgctaatcagtttctgttcTCCACCTTTAAAATAAGTGAAAAATTG
1565	ATGATTgcgAAATACACTGTATTATATACATC
1566	CAGTGTATTTcgcAATCATAATATTATTAATTTTTATT
1567	GCATTCgcgTTGAACGGAGATATGCTAAG
1568	CGTTCAAcgcGAATGCAACATACGG
CS3-for	gatggaTCCCATGAAAATACGCACGCG
CS3-rev	GTGGAATTCCTCGCACACAGAGGG
nlpA-F1	gcaggaTCCCACGCTTCATCTGATAATGACG
nlpA-r1	GCAGAATTCCGGCCAGCAATAATG